

Excess Thermodynamics of Mixtures Involving Xenon and Light Linear Alkanes by Computer Simulation

A. J. Palace Carvalho,^{*,†} J. P. Prates Ramalho,[‡] and Luís F. G. Martins[†]

Centro de Química de Évora, Universidade de Évora, Rua Romão Ramalho 59, 7000-671 Évora, Portugal, and Centro de Física Teórica e Computacional, Avenida Prof. Gama Pinto 2, 1649-003 Lisboa Codex, Portugal

Received: February 2, 2007; In Final Form: March 22, 2007

Excess molar enthalpies and excess molar volumes as a function of composition for liquid mixtures of xenon + ethane (at 161.40 K), xenon + propane (at 161.40 K) and xenon + *n*-butane (at 182.34 K) have been obtained by Monte Carlo computer simulations and compared with available experimental data. Simulation conditions were chosen to closely match those of the corresponding experimental results. The TraPPE-UA force field was selected among other force fields to model all the alkanes studied, whereas the one-center Lennard–Jones potential from Bohn et al. was used for xenon. The calculated H_m^E and V_m^E for all systems are negative, increasing in magnitude as the alkane chain length increases. The results for these systems were compared with experimental data and with other theoretical calculations using the SAFT approach. An excellent agreement between simulation and experimental results was found for xenon + ethane system, whereas for the remaining two systems, some deviations that become progressively more significant as the alkane chain length increases were observed.

1. Introduction

The thermodynamics of mixtures involving rare gases and alkanes has become a field of increasing interest in the last two decades. In particular, systems of xenon + alkane type have been attracting the most interest from researchers for both practical and fundamental reasons. Xenon is a hydrophobic solute with anaesthetic properties at subatmospheric pressures, and the study of the interactions of xenon with alkylic chains can give a contribution to elucidate some aspects of the general mechanism of anaesthesia, which is not yet completely understood.¹ In fact, according to some of the most recent studies, the anaesthetic action of xenon could be a result of a nonspecific interaction between xenon and either the alkylic chains of the cellular membrane or some hydrophobic (alkylic) pocket inside a membrane protein.² On the other hand, xenon and the alkanes (and their mixtures) have long been used to test the theories of liquid state. Xenon, being a spherical, structureless and polarizable particle, is the perfect choice as a common component of any series of systems in which the differences introduced by a second component are to be devised; alkanes constitute a family of compounds whose properties vary regularly through the homologous series.³ These characteristics make mixtures of xenon and the alkanes suited to study the role of size and shape on the thermodynamic properties of liquid mixtures.

The systematic study of the mixtures of xenon with the alkanes was initiated after the surprising results found for the system xenon + ethane: the four main excess functions (G_m^E , V_m^E , H_m^E , and S_m^E) for the system were negative, and this was the first time that such behavior was observed in mixtures of simple liquids.⁴ By measurements of vapor pressures for this system at several temperatures, Nunes da Ponte et al.⁵ have

confirmed that the system exhibits negative deviations from Raoult's law up to the critical line. Those results, suggesting a strong attraction between xenon (a rare gas) and ethane (an alkane) in the absence of permanent dipole moments or association were not explained by the existing theories of liquid mixtures at that time (perturbation theory of Gray and Gubbins^{6,7}).

The negative values of V_m^E and H_m^E for xenon + ethane mixtures can also, however, be obtained using the correlations from the work of Singer and Singer⁸ if both xenon and ethane are modeled by one-center Lennard–Jones potentials with the parameters adjusted by fitting of the vapor pressures and densities of the pure compounds.⁴

The system xenon + propane is the most natural choice to follow in the study of the interaction between xenon and alkylic chains. In that case, G_m^E and V_m^E are also negative with higher absolute values, as expected from the differences in free volumes between the components. The values of G_m^E and V_m^E for the system xenon + butane, studied in sequence, follow the same trend observed in the previous two.⁹ At this point, it became apparent that the behavior of the systems of type xenon + alkane resembles that of systems of type alkane + alkane. In the case of H_m^E , it would be interesting to investigate if xenon + alkane mixtures exhibit the main characteristics showed by mixtures of alkanes, i.e., a decreasing tendency of H_m^E with increasing temperature until it crosses the $H_m^E = 0$ axis as a sigmoid curve (as a function of composition) and eventually becoming negative.³ Despite the fact that the H_m^E for the system xenon + ethane is negative, the estimated H_m^E for the equimolar mixture of the system xenon + propane, obtained from the G_m^E ($x = 0.5$) dependence on temperature using the Gibbs–Helmholtz relation, is positive.⁴ The same estimation for xenon + butane gives a value close to zero.⁹

Systems involving xenon and alkanes have also been treated theoretically using some versions of the statistical associating

* To whom correspondence should be addressed. E-mail: ajpalace@uevora.pt.

[†] Universidade de Évora.

[‡] Centro de Física Teórica e Computacional.

fluid theory (SAFT) approach,^{4,9,10} which became one of the most successful predictive tools for phase diagrams and, more recently, of excess properties of this kind of systems. Moreover, using the SAFT, along with a close inspection of several properties of alkanes and xenon, at both microscopic and macroscopic levels, it was shown that the behavior of xenon correlates very well with that of the alkanes.^{9,11}

Molecular simulation of fluid systems has become an increasingly important tool for predicting thermodynamic properties of liquids and liquid mixtures, being nowadays applied to a wide variety of systems, owing to the rapid development of high-speed computers. In the setting up of a molecular simulation, the choice of the force field that models the molecular interactions is central to the quality of the results that will be produced by the calculations. Over the past few years, a significant number of force fields for linear and branched alkanes have been proposed. Those force fields have been applied to the prediction of phase diagrams^{12–14} and, to a much less extent, excess properties.¹⁵ Since the molecular simulation results are “experimental” for the particular force field chosen, their comparison with theory can be used to test the latter, and a comparison with experimental results can be used to test the force field. In the case of systems involving xenon and the light alkanes in C₂, C₃, and C₄, excess properties have been determined experimentally and calculated by both the perturbation theory of Bohn and Lustig¹⁶ and the SAFT,^{4,9} but to our knowledge, no simulation results have been available until now.

In this work, excess volumes and excess enthalpies were calculated for binary mixtures of xenon + ethane, xenon + propane, and xenon + *n*-butane by Monte Carlo simulation and, whenever possible, compared with experimental results. The force fields used in the simulations were selected among the several possibilities using as a quality criterion the best description of the temperature dependence of pure component densities.

2. Simulation Details

The computer simulations of the xenon–alkane liquid mixtures were calculated by the Monte Carlo method in the isothermal–isobaric (NPT) ensemble using the MCCCSTowhee Monte Carlo molecular simulation package, version 4.15.3.¹⁷

For each of the three alkanes studied (ethane, propane, and *n*-butane), a series of simulations were performed in which the proportions of molecules of each component of the binary mixture were varied. Each simulated mixture consisted of a total number of between 300 and 500 molecules so as to fill a cubic box of ~30 Å each side at the mixture’s density. The temperatures of 161.40 K (for ethane and propane) and 182.34 K (for *n*-butane) and the experimental vapor pressure of each mixture at the respective temperature were chosen as the simulation conditions to closely match the experimental conditions under which the available experimental data of the analogous systems^{4,9} were obtained. It should be noted that the available experimental H_m^E for the xenon + ethane mixture was determined at 163 K, which differs by 1.6 K from the temperature at which the corresponding simulation was performed. However, it is believed that this small temperature difference should not have any significant influence in any deviation that may be observed between the two sets of data. A summary of the specified simulation conditions is presented in Table 3.

In each simulation, a preliminary equilibration run of 50 000 steps (in which each step consists of a number of movements

TABLE 1: Parameters of United-Atom Intermolecular Interactions

	Lennard–Jones parameters	
	ϵ/K	$\sigma/\text{Å}$
CH ₃	98.	3.75
CH ₂	46.	3.95
Xe	227.8557	3.9478

TABLE 2: Parameters of Alkane Intramolecular Interactions

	intramolecular parameters	
	bond terms	r_0
angle terms	c_1	31 250 K/rad ²
	θ_0	114°
torsion terms	c_1	355.03 K
	c_2	–68.19 K
	c_3	791.32 K

equal to the number of molecules in the system) was followed by a production run for the calculation of averages consisting of another 100 000 steps, which were divided into 20 blocks in order to estimate errors. Shorter production runs would be sufficient for the calculation of other molar thermodynamic properties that can be obtained directly from a single simulation. However, excess functions are by their nature very affected by larger statistical errors because they are small differences of large quantities affected by uncertainties of orders of magnitude similar to those differences. It is not infrequent that the errors affecting the calculated excess properties are of the same order of magnitude or even exceed the values of the properties themselves.

The Monte Carlo moves consisted of simulation box volume changes, coupled–decoupled configurational-bias regrowths,¹⁸ translations of the center of mass, and rotations about the center of mass. Additionally, to improve the convergence for longer-chain molecules (propane and butane), configurational-bias molecule reinsertions in the simulation box and aggregation volume-bias moves^{19,20} were also applied.

The alkane molecules were modeled by the united-atom version of the TraPPE force field, developed for the simulation of phase equilibria of hydrocarbons by Siepmann and co-workers.²¹ Other force fields were tested; namely, the Gromos,²² the OPLS,²³ and the NERD (version 3),²⁴ but the TraPPE-UA force field was found to give the best agreement between calculated and experimental pure density data for these particular systems. This force field uses fixed bond lengths, harmonic style angle bending terms, and quadratic torsion terms for the intramolecular interactions. The intermolecular terms are modeled by Lennard–Jones potentials. The xenon atoms were modeled by a Lennard–Jones potential with parameters obtained by Bohn and co-workers.²⁵ This is an effective potential whose parameters were obtained on the basis of the experimental density of xenon. For the xenon–alkane interactions, the L–J parameters were obtained by Lorentz–Berthelot mixing rules. A 15 Å cutoff radius was used in the calculations of the interactions, and the neglect of long range interactions beyond the cutoff radius was compensated by applying analytic tail corrections. No calculations of Coulombic interactions were performed, since all the molecules studied are neutral and apolar. All the parameters of the potentials used are presented in Tables 1 and 2.

The calculated excess properties (excess molar volume and excess molar enthalpy) were obtained from the calculated molar

TABLE 3: Specified Conditions for the Series of Simulations of Xenon–Alkane Liquid Mixtures (and the Pure Liquids, As Well)

	x_{Xe}	N_{Xe}	N_{A}	N_{total}	p/kPa	T/K
xenon + ethane	0.00	0	400	400	23.67	161.40
	0.22	87	313	400	35.08	
	0.38	153	247	400	44.40	
	0.50	200	200	400	51.28	
	0.52	206	194	400	52.17	
	0.64	255	145	400	59.59	
	0.81	322	78	400	69.94	
	1.00	500	0	500	81.663	
xenon + propane	0.00	0	300	300	0.946	161.40
	0.17	50	250	300	13.685	
	0.37	147	253	400	29.184	
	0.50	200	200	400	39.800	
	0.52	209	191	400	41.577	
	0.64	256	144	400	51.489	
	0.80	318	82	400	64.665	
	1.00	500	0	500	81.663	
xenon + butane	0.00	0	300	300	0.423	182.34
	0.22	66	234	300	48.27	
	0.37	147	253	400	82.15	
	0.50	200	200	400	115.6	
	0.55	220	180	400	128.12	
	0.66	262	138	400	156.47	
	0.81	325	75	400	198.33	
	1.00	500	0	500	248.22	

TABLE 4: Molar Volumes for the Simulated Pure Liquids

system	$V_{\text{m}}/\text{cm}^3 \text{ mol}^{-1}$
xenon at 161.40K	44.14 ± 0.02
xenon at 182.34K	46.36 ± 0.02
ethane at 161.40K	52.64 ± 0.03
propane at 161.40K	66.91 ± 0.02
<i>n</i> -butane at 182.34 K	83.91 ± 0.03

TABLE 5: Excess Enthalpies and Excess Volumes for Xenon + Ethane Mixtures at 161.40 K

x_{Xe}	$H_{\text{m}}^{\text{E}}/\text{J mol}^{-1}$	$V_{\text{m}}^{\text{E}}/\text{cm}^3 \text{ mol}^{-1}$
0	0 ± 13.7	0 ± 0.046
0.2175	-26.9 ± 12.9	-0.058 ± 0.042
0.3825	-41.4 ± 14.0	-0.090 ± 0.045
0.5000	-49.7 ± 10.0	-0.116 ± 0.032
0.5150	-46.2 ± 12.2	-0.107 ± 0.038
0.6375	-48.8 ± 14.1	-0.121 ± 0.044
0.8050	-32.2 ± 9.24	-0.072 ± 0.029
1	0 ± 10.3	0 ± 0.031

properties of the pure liquids and each mixture according to the equations

$$V^{\text{E}} = V_{\text{mixture}} - x_{\text{Xe}}V_{\text{Xe}}^* - x_{\text{A}}V_{\text{A}}^*$$

$$H^{\text{E}} = H_{\text{mixture}} - x_{\text{Xe}}H_{\text{Xe}}^* - x_{\text{A}}H_{\text{A}}^*$$

where the index A denotes the alkane and the superscripted star stands for a pure substance property. The enthalpies were calculated from the average total energies, average volumes, and specified ensemble pressures.

$$H = \langle U \rangle_{\text{NPT}} + P \langle V \rangle_{\text{NPT}}$$

3. Results and Discussion

Excess Properties. In Table 4, the molar volumes of pure xenon, ethane, propane, and *n*-butane are presented as determined in the simulations of the pure liquids (see Table 3 for the conditions for the simulations).

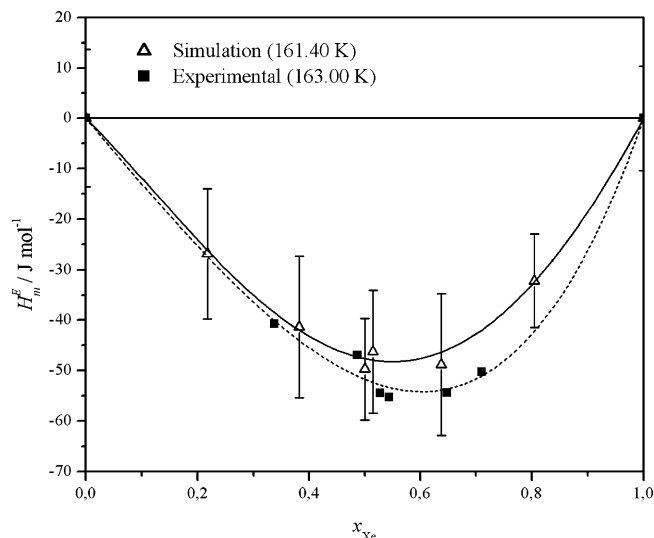


Figure 1. Excess molar enthalpies for xenon + ethane at 161.40 K. The filled squares represent the experimental results at 163.0 K (with dashed line representing the corresponding Redlich–Kister fitting), and the open triangles represent the simulation results from this work (solid line for Redlich–Kister fitting). The error bars of simulation results are also shown.

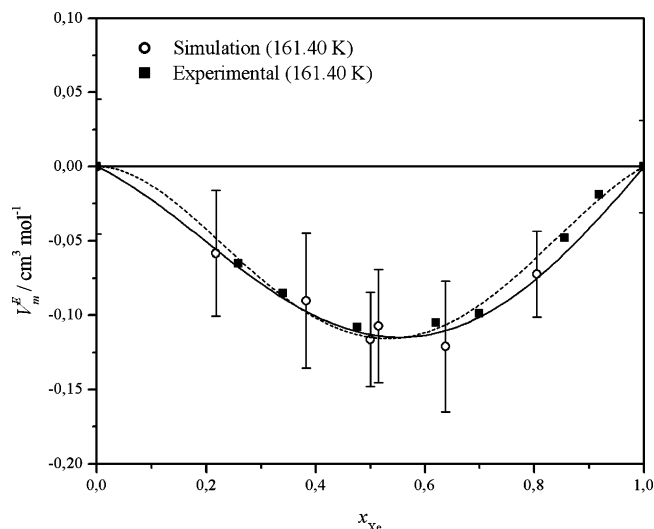


Figure 2. Excess molar volumes for xenon + ethane at 161.40 K. The solid squares represent the experimental results (with dashed line representing the corresponding Redlich–Kister fitting), and the open circles represent the simulation results from this work (solid line for Redlich–Kister fitting). The error bars of simulation results are also shown.

The excess molar enthalpies and excess molar volumes of the system xenon + ethane at 161.40 K were calculated for the xenon mole fractions of 0, 0.2175, 0.3825, 0.5000, 0.5150, 0.6375, 0.8050, and 1, and the results are presented in Table 5. H_{m}^{E} and V_{m}^{E} as functions of composition are plotted in Figures 1 and 2, respectively. The results were calculated at saturation pressures. Because of the low pressures involved, the calculated excess enthalpy and excess volume values were not corrected to zero pressure, since the corrections would be well within the calculation statistical errors. To obtain a better definition of the dependence of each excess function on the composition, the calculated results were fitted to Redlich–Kister-type equations,

$$\frac{H_{\text{m}}^{\text{E}}}{RTx(1-x)} = \sum_{k=0}^n A_k(1-2x)^k \quad (1)$$

TABLE 6: Excess Enthalpies and Excess Volumes for Xenon + Propane Mixtures at 161.40 K

x_{Xe}	$H_m^E/\text{J mol}^{-1}$	$V_m^E/\text{cm}^3 \text{mol}^{-1}$
0	0 ± 8.6	0 ± 0.024
0.1667	-2.42 ± 9.1	-0.0180 ± 0.025
0.3675	-29.1 ± 7.7	-0.0952 ± 0.023
0.5000	-37.7 ± 9.8	-0.124 ± 0.029
0.5225	-54.8 ± 8.6	-0.170 ± 0.025
0.6400	-54.2 ± 10.6	-0.166 ± 0.031
0.7950	-33.4 ± 10.7	-0.112 ± 0.034
1	0 ± 10.8	0 ± 0.034

for excess enthalpy and

$$\frac{V_m^E}{x(1-x)} = \sum_{k=0}^n B_k(1-2x)^k \quad (2)$$

for excess volume, where x is the mole fraction of the more volatile component, and the resulting parameters are recorded in Table 8. Both H_m^E and V_m^E are negative in the whole composition range, being slightly asymmetric, with the minimum value shifted toward mole fractions richer in the more volatile component. The simulation results are compared to experimental ones from Filipe et al.⁴ in Figures 1 and 2. The agreement between calculated and experimental values is excellent for both V_m^E and H_m^E , as the simulation model describes the sign, the magnitude, and even the asymmetry of these excess properties as a function of composition. The calculated values for the equimolar mixtures are also in close agreement with the figures obtained in the work mentioned above [the calculated $H_m^E(x=0.5) = -49.7 \text{ J mol}^{-1}$ at 161.40 K, as compared with the experimental $H_m^E(x=0.5) = -51.7 \text{ J mol}^{-1}$ at 163.00 K, and the calculated $V_m^E(x=0.5) = -0.116 \text{ cm}^3 \text{mol}^{-1}$, as compared with the experimental $V_m^E(x=0.5) = -0.115 \text{ cm}^3 \text{mol}^{-1}$, both at 161.40 K].

For the system xenon + propane, the excess molar enthalpies and the excess molar volumes were calculated for the xenon mole fractions of 0, 0.1667, 0.3675, 0.5000, 0.5225, 0.6400, 0.7950, and 1 at 161.4 K, and the results are recorded in Table 6. H_m^E vs x and V_m^E vs x are plotted in Figures 3 and 4, respectively. Just as well as in the case of the xenon + ethane system, the data calculated at saturation pressure was not corrected to zero pressure. They were also fitted to Redlich–Kister-type eqs 1 and 2, the parameters being recorded in Table 8. For the xenon + propane mixtures, the V_m^E as a function of composition is also negative with a slight asymmetry and can also be compared with the experimental results from Filipe et al.⁴ in Figure 4. The sign, the order of magnitude, and the asymmetry are well-predicted, the calculated values being less negative than the experimental ones. The calculated $V_m^E(x=0.5)$ was found to be $-0.124 \text{ cm}^3 \text{mol}^{-1}$ (cf. experimental $V_m^E(x=0.5) = -0.308 \text{ cm}^3 \text{mol}^{-1}$). The values of H_m^E are also negative and larger in magnitude than those for xenon + ethane mixtures. There are no experimental results of H_m^E for this system; however, Filipe et al.⁴ estimated from the temperature dependence of $G_m^E(x=0.5)$ an average value of $H_m^E(x=0.5)$ in the range 161.4–195.48 K, which was found to be 140 J mol^{-1} .

In the case of the system xenon + butane, the results are qualitatively similar to the previous systems. The excess molar enthalpies and excess molar volumes, calculated for the xenon mole fractions of 0, 0.2200, 0.3675, 0.5000, 0.5500, 0.6550, 0.8125, and 1 at 182.34 K, are recorded in Table 7 and plotted in Figure 3 and 5, respectively. As well as for the other systems,

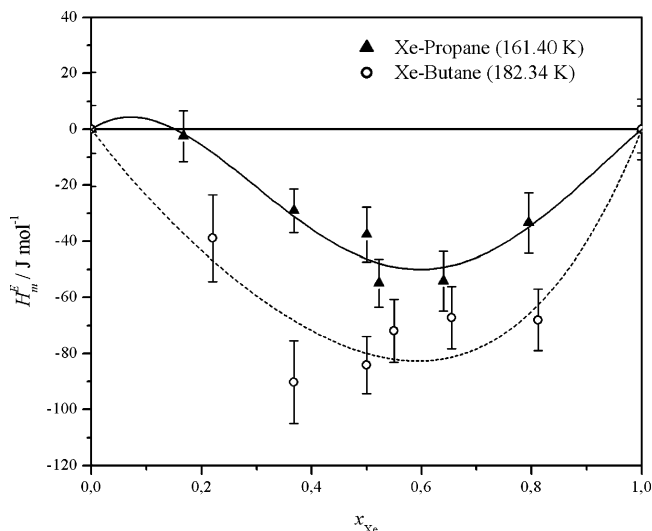


Figure 3. Excess enthalpies for xenon + propane at 161.40 K (solid triangles) and for xenon + butane at 182.34 K (open circles). The curves are the corresponding Redlich–Kister fittings (solid line for xenon + propane and dashed line for xenon + butane). The error bars of simulation results are also shown.

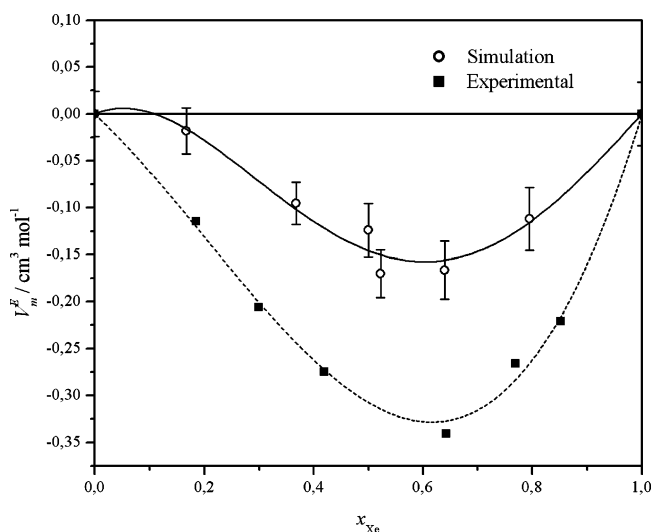


Figure 4. Excess molar volumes for xenon + propane at 161.40 K. The solid squares represent the experimental results (with dashed line representing the corresponding Redlich–Kister fitting), and the open circles represent the simulation results from this work (solid line for Redlich–Kister fitting). The error bars of simulation results are also shown.

TABLE 7: Excess Enthalpies and Excess Volumes for Xenon + Butane Mixtures at 182.34 K

x_{Xe}	$H_m^E/\text{J mol}^{-1}$	$V_m^E/\text{cm}^3 \text{mol}^{-1}$
0	0 ± 20.4	0 ± 0.042
0.2200	-38.9 ± 15.5	-0.220 ± 0.034
0.3675	-90.3 ± 14.7	-0.414 ± 0.037
0.5000	-84.2 ± 10.2	-0.418 ± 0.029
0.5500	-71.9 ± 11.3	-0.395 ± 0.032
0.6550	-67.2 ± 11.1	-0.395 ± 0.032
0.8125	-68.0 ± 10.0	-0.354 ± 0.036
1	0 ± 8.4	0 ± 0.031

no pressure corrections were needed, and the simulation results were fitted to eqs 1 and 2, whose parameters are shown in Table 8. One can see that V_m^E is negative and almost quadratic. A comparison can be made with experimental results from Filipe et al.⁹ The simulation predicts the sign of the excess property and the shape of the V_m^E dependence on composition.

TABLE 8: Coefficients of Redlich–Kister Eqs 1 and (2) Applied to Calculated V_m^E and V_m^E Results of Xenon + Ethane, Xenon + Propane, and Xenon + Butane

coefficient	system		
	xenon + ethane $T = 161.40$ K	xenon + propane $T = 161.40$ K	xenon + butane $T = 182.34$ K
A_0	-0.142	-0.138	-0.211
A_1	0.0342	0.111	0.0743
A_2	0.0252	0.125	-0.0344
B_0	-0.452	-0.583	-1.65
B_1	0.134	0.444	0.661
B_2	0.150	0.388	-0.435

Its magnitude is, however, not well-predicted, the calculated values being about one-half of the experimental ones near the minimum [calculated $V_m^E(x = 0.5) = -0.418 \text{ cm}^3 \text{ mol}^{-1}$, in comparison with the experimental $V_m^E(x = 0.5) = -0.806 \text{ cm}^3 \text{ mol}^{-1}$]. The values of H_m^E are also negative and larger in magnitude than those for xenon + propane mixtures. There are also no experimental results of H_m^E for this system. As for the previous system, Filipe et al.⁹ estimated an average value of $H_m^E(x = 0.5) = 17 \text{ J mol}^{-1}$ in the range 182.34–195.48 K.

Simulation describes the experimental descending trend for the values of V_m^E at the equimolar composition in the series xenon + ethane, propane, butane. This trend is also apparent for the calculated results of the equimolar H_m^E ; however, the sign of the experimental values of H_m^E is not reproduced in the case of the systems xenon + propane and xenon + butane. For the latter, the experimental figure is essentially zero within the experimental error; however, it must be stressed that, since the values of H_m^E for systems xenon + propane and xenon + butane were obtained from the experimental G_m^E by differentiation, the errors of these values are typically larger than those obtained by direct experimental measurement. The positive equimolar H_m^E found for these two systems (in fact, almost zero in the case of xenon + butane) has been thought to belong to a broader trend of mixtures involving only alkanes, since there is a resemblance between xenon and alkanes from a thermodynamic point of view.^{9,11} It has been observed that the H_m^E of systems involving alkanes is positive at sufficiently high temperatures, and as the temperature rises, H_m^E decreases until it crosses the $H_m^E = 0$ axis as a sigmoid curve (as a function of composition) and eventually becomes negative. Martins¹⁶ has shown that although the temperature at which $H_m^E(x = 0.5)$ passes through 0 is different from system to system, the corresponding reduced temperature at which it occurs presents an interesting constancy around 0.57–0.58. Following the hypothesis that the behavior of xenon + alkane systems is similar to that of alkane + alkane systems, it was noted that, in fact, the reduced temperature at which the H_m^E of xenon + propane system was obtained was below 0.57–0.58 (and, therefore, the equimolar H_m^E should be positive at this temperature), and this temperature for xenon + butane system was nearly 0.57 (which indicates that it should be 0, as it roughly is, as determined experimentally). However, in the case of ethane, the results do not follow this trend: although the reduced temperature is well below 0.57–0.58, $H_m^E(x = 0.5)$ is already negative at this temperature. That fact suggests two possible interpretations. On one hand, the xenon + ethane could be an exception to a general rule exhibited by xenon + alkane mixtures, which would be due to the fact that ethane (and even more so in the case of methane) departs slightly from the general trends shown by pure component properties of *n*-alkanes.⁴ On the other hand, since the results for xenon + ethane are the

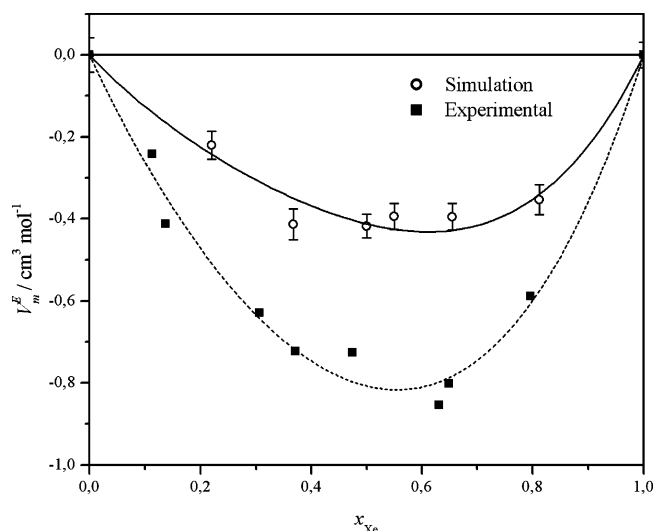


Figure 5. Excess molar volumes for xenon + butane at 182.34 K. The solid squares represent the experimental results (with dashed line representing the corresponding Redlich–Kister fitting), and the open circles represent the simulation results from this work (solid line for Redlich–Kister fitting). The error bars of simulation results are also shown.

only ones that were obtained directly from experiment, it could also be argued that systems involving xenon and the lightest alkanes cannot be integrated in the general behavior of higher alkanes mixtures, or even if showing a similar behavior, it could result in a different value of temperature at which $H_m^E(x = 0.5) = 0$. The simulation results obtained in this work (negative H_m^E for both xenon + propane and xenon + butane) seem to corroborate the latter conclusion. A more detailed analysis would require simulation results of H_m^E for these three systems at more temperatures and (even more importantly) experimental results of H_m^E as a function of temperature, which are ongoing and will be the subject of future publications.

Recently, dos Ramos et al.²⁶ obtained excess molar enthalpies, excess molar volumes, and excess Gibbs free energies for xenon + propane and xenon + butane using the soft-SAFT approach.²⁷ In Table 9, the theoretical predictions from dos Ramos et al. are compared with the present results and experimental data for the equimolar excess functions studied. As can be seen, simulation data and SAFT predictions deviate from experimental results in the same qualitative way for the systems xenon + propane and xenon + butane, the SAFT values being closer to the experiment than the simulation data. As a matter of fact, the model behind the SAFT approach, especially after the corrections for the effect of conformational changes upon mixing,²⁸ and the united atom TraPPE force field are models that are formally very close to each other, leading naturally to results in close agreement.

Solution Structure. The solution structure was characterized by the group–group radial distribution functions $g_{ab}(r)$, which represent the probability density of the occurrence of a group of type “a” (united atom) at a distance r from groups of type “b”. Figures 6–10 show the comparison among the group–group radial distribution functions for three different group combinations (CH_3/CH_3 , Xe/CH_3 and Xe/Xe) in the three mixtures. The $g_{ab}(r)$ for the xenon–butane mixture are presented separately because those simulations were performed at a different temperature.

In general, it can be observed from the comparison among the several $g_{ab}(r)$ that for all the systems, the Xe/Xe peak is always the narrowest one, followed by the Xe/CH_3 and the $\text{CH}_3/$

TABLE 9: Comparison between Excess Molar Enthalpies and Excess Molar Volumes for the Equimolar Mixture Obtained by Simulation, SAFT Approach, and Experimental Data

system	T/K	$H_m^E(x=0.5)/J\ mol^{-1}$			$V_m^E(x=0.5)/cm^3\ mol^{-1}$		
		exptl	simul ^a	SAFT ^b	exptl	simul ^a	SAFT ^b
xenon + ethane	161.40		-49.7		-0.115 ^c	-0.116	
	163.0	-51.7 ^c					
xenon + propane	161.40		-37.7	-12.9	-0.308 ^c	-0.124	-0.225
	182.34	140 ^c		-20.9			-0.301
	195.49			-25.3			-0.365
xenon + butane	182.34	17 ^d	-84.2	-49.2	-0.806 ^d	-0.418	-0.582
	195.49			-42.6			-0.705

^a This work. ^b Ref 26. ^c Ref 4. ^d Ref 9.

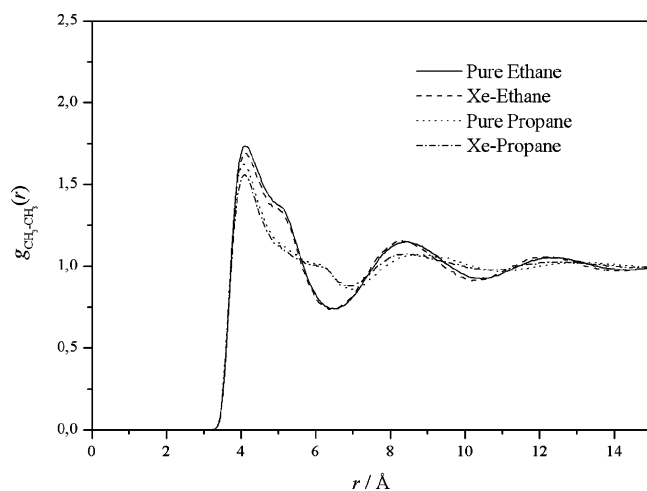


Figure 6. Comparison between the CH_3/CH_3 radial distribution functions of the xenon + ethane (dashed line) and xenon + propane (dashed-dotted line) equimolar mixtures and of the pure ethane (solid line) and propane (dotted line) liquids ($T = 161.4\ K$).

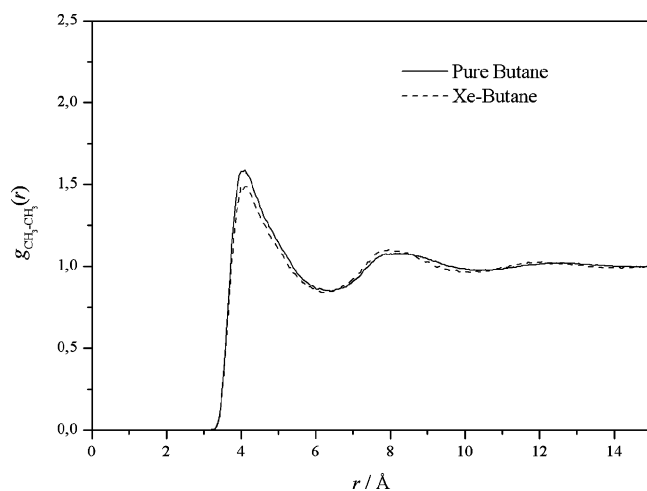


Figure 7. Comparison between the CH_3/CH_3 radial distribution functions of the xenon + butane (dashed line) equimolar mixture and of the pure butane (solid line) liquid ($T = 182.34\ K$).

CH_3 , the former appearing at larger distances than the other two, reflecting the relative differences in the diameters of the groups.

For the shorter alkanes, the CH_3/CH_3 first peaks present noticeable shoulders (Figure 6) that correspond to the second CH_3 group of each molecule. Due to the longer chain length of butane and, consequently, the wider variety of conformations, this shoulder fades away in the case of this alkane (Figure 7). For all cases, the pure alkane distribution functions have a somewhat higher first peak in comparison with the corresponding distribution functions of the mixtures.

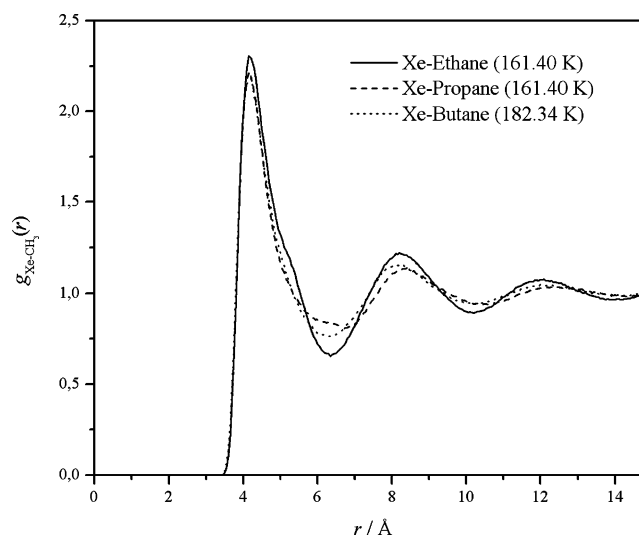


Figure 8. Comparison between the Xe/CH_3 radial distribution functions of the xenon + ethane (solid line), xenon + propane (dashed line), and xenon + butane (dotted line) equimolar mixtures.

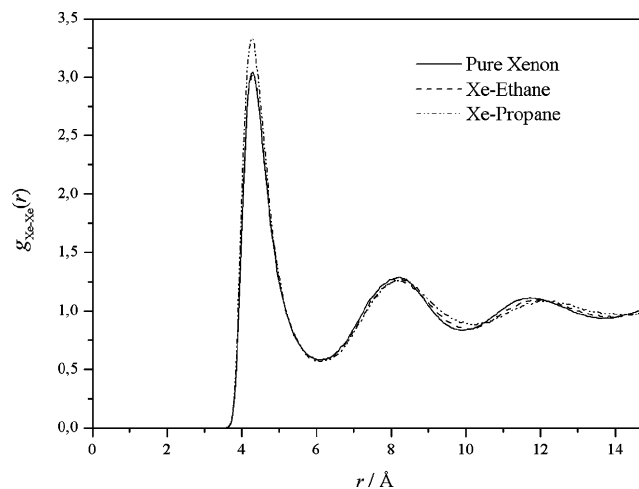


Figure 9. Comparison between the Xe/Xe radial distribution functions of the xenon + ethane (dashed line) and xenon + propane (dashed-dotted line) equimolar mixtures and of the pure xenon (solid line) liquid ($T = 161.4\ K$).

The Xe/CH_3 peaks appear roughly at the same value of r for all the systems (Figure 8); however, xenon seems to be more populated by CH_3 in the first coordination sphere in mixtures with ethane than when mixed with the other two alkanes. This observation is not surprising, considering that for the propane and butane systems, the CH_2 groups will also populate the first coordination sphere and therefore diminish the residence of the CH_3 groups around xenon.

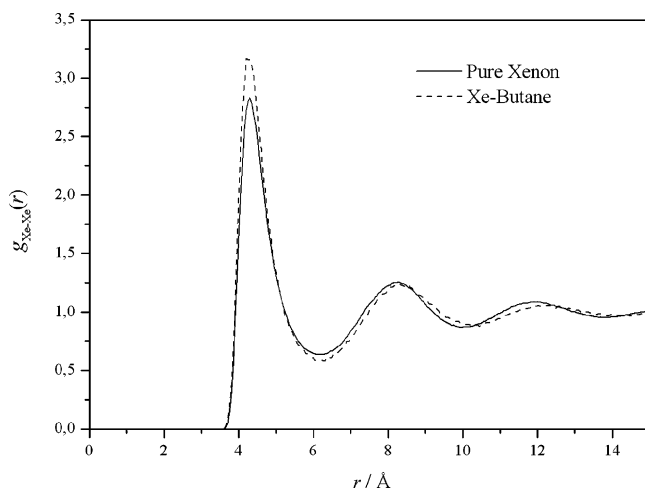


Figure 10. Comparison between the Xe/Xe radial distribution functions of the xenon + butane (dashed line) equimolar mixture and of the pure xenon (solid line) liquid ($T = 182.34$ K).

For the xenon–ethane mixture, the Xe/CH₃ first peak also presents a small shoulder due to the second CH₃ group of the ethane molecule. This is, however, less noticeable in this distribution function than it is in the CH₃/CH₃ case (Figure 6). For the other mixtures, this shoulder is indistinguishable from the baseline.

In Figures 9 and 10, one can observe a remarkable resemblance in the Xe/Xe distribution functions of both the pure xenon and the xenon–alkane mixtures. At longer ranges, however, the mixtures are somewhat less structured. A striking feature is a higher first peak in the mixtures' distribution functions in comparison with those of pure xenon (Figures 9 and 10), with the exception of the xenon–ethane $g_{ab}(r)$, for which the first peak is almost coincident with the pure xenon one. The larger alkane molecules seem to exert a “compressive” action on the first coordination sphere, which hinders the mobility of the xenon atoms.

4. Conclusions

Excess molar enthalpies and excess molar volumes as functions of composition for the liquid binary mixtures of xenon and the light linear alkanes ethane, propane, and *n*-butane have been obtained by Monte Carlo computer simulations in the (NPT) ensemble. The calculated H_m^E and V_m^E for all the systems are negative, increasing in magnitude as the alkane chain length increases. The comparison between the simulation results and available experimental data was excellent for the xenon + ethane mixture in the case of both the molar excess volumes and the molar excess enthalpies. For the other two mixtures, some deviations were observed between simulation and experimental results, with the simulated excess molar volume curve becoming

less negative than the experimental one as the alkane chain length increases. In the case of the excess molar enthalpy, the positive sign obtained by indirect methods in experimental studies is not predicted by the present simulations.

Acknowledgment. We thank E. J. M. Filipe and co-workers for sharing with us some preliminary unpublished results of their ongoing research and for fruitful discussions about this subject. We also thank Fundação para a Ciência e Tecnologia and FEDER for financial support through research project POCTI/QUI/46299/2002.

References and Notes

- (1) Lynch, C., III; Baum, J.; Tenbrinck, R. *Anesthesiology* **2000**, *92*, 865.
- (2) Trudell, J. R.; Koblin, D. D.; Eger, E. I., II *Anesth. Analg.* **1998**, *87*, 411.
- (3) Rowlinson, J. S.; Swinton, F. L. *Liquids and Liquid Mixtures*, 3rd ed.; Butterworth Scientific: London, 1982.
- (4) Filipe, E. J. M.; Gomes de Azevedo, E. J. S.; Martins, L. F. G.; Soares, V. A. M.; Calado, J. C. G.; McCabe, C.; Jackson, G. *J. Phys. Chem. B* **2000**, *104*, 1315.
- (5) Nunes da Ponte, M.; Chokappa, D.; Calado, J. C. G.; Clancy, P.; Streett, W. B. *J. Phys. Chem.* **1985**, *89*, 2746.
- (6) Twu, C. H.; Gubbins, K. E.; Gray, C. J. *Mol. Phys.* **1975**, *29*, 713.
- (7) Gubbins, K. E.; Gray, C. G.; Machado, J. R. S. *Mol. Phys.* **1981**, *42*, 817.
- (8) Singer, J. V. L.; Singer, K. *Mol. Phys.* **1972**, *25*, 251.
- (9) Filipe, E. J. M.; Martins, L. F. G.; Calado, J. C. G.; McCabe, C.; Jackson, G. *J. Phys. Chem. B* **2000**, *104*, 1322.
- (10) Dias, L. M. B.; Filipe, E. J. M.; McCabe, C.; Calado, J. C. G. *J. Phys. Chem.* **2004**, *108*, 7377.
- (11) Filipe, E. J. M.; Dias, L. M. B.; Calado, J. C. G.; McCabe, C.; Jackson, G. *Phys. Chem. Chem. Phys.* **2002**, *4*, 1618.
- (12) Stubbs, J. M.; Chen, B.; Potoff, J. J.; Siepmann, J. I. *Fluid Phase Equilib.* **2001**, *301*, 183–184.
- (13) Serbanovic, S. P.; Mijajlovic, M. L.; Radovic, I. R.; Djordjevic, B. D.; Kijevcanin, M. L.; Djordjevic, E. M.; Tasic, A. Z. *J. Serb. Chem. Soc.* **2005**, *70*, 527.
- (14) McKnight, T. J.; Vlugt, T. J. H.; Ramjugernath, D.; Starzak, M.; Ahlstrom, P.; Bolton, K. *Fluid Phase Equilib.* **2005**, *232*, 136.
- (15) Wallis, E. P. *Fluid Phase Equilib.* **1995**, *103*, 97.
- (16) Martins, L. F. G. Ph.D. Thesis, Instituto Superior Técnico, Lisbon, 1999.
- (17) Martin, M. G. *MCCCS Towhee*. Available at: <http://towhee.sourceforge.net/>.
- (18) Martin, M. G.; Siepmann, J. I. *J. Phys. Chem. B* **1999**, *103*, 4508.
- (19) Chen, B.; Siepmann, J. I. *J. Phys. Chem. B* **2000**, *104*, 8725.
- (20) Chen, B.; Siepmann, J. I. *J. Phys. Chem. B* **2001**, *105*, 11275.
- (21) Martin, M. G.; Siepmann, J. I. *J. Phys. Chem. B* **1998**, *102*, 2569.
- (22) Scott, W. R. P.; Hunenberger, P. H.; Tironi, I. G.; Mark, A. E.; Billeter, S. R.; Fennen, J.; Torda, A. E.; Huber, T.; Kruger, P.; van Gunsteren, W. F. *J. Phys. Chem. A* **1999**, *103*, 3596.
- (23) Kaminski, G. A.; Friesner, R. A.; Tirado-Rives, J.; Jorgensen, W. L. *J. Phys. Chem. B* **2001**, *105*, 6474.
- (24) Khare, R.; Sum, A. K.; Nath, S. K.; de Pablo, J. J. *J. Phys. Chem. B* **2004**, *108*, 10071.
- (25) Bohn, M.; Lago, S.; Fischer, J.; Kohler, F. *Fluid Phase Equilib.* **1985**, *23*, 137.
- (26) Ramos, M. C.; Blas, F. J.; Filipe, E. J. M. Unpublished results, available with kind permission by the authors.
- (27) Blas, F. J. *Mol. Phys.* **2002**, *100*, 2221.
- (28) Blas, F. J.; Vega, L. F. *Ind. Eng. Chem. Res.* **1998**, *37*, 660.